Received: 19 November 2020 | Revised: 3 January 2021 | Accepted: 4 January 2021

DOI: 10.1002/jcla.23706

RESEARCH ARTICLE

WILEY

GC-MS metabolomics identifies novel biomarkers to distinguish tuberculosis pleural effusion from malignant pleural effusion

Yongxia Liu[1] | Bin Mei[1] | Deying Chen[2] | Long Cai[1]

[1]Affiliated Hangzhou Chest Hospital, Zhejiang University School of Medicine, Hangzhou, China

[2]The First Affiliated Hospital, School of Medicine, Zhejiang University, Hangzhou, China

Correspondence
Long Cai, Affiliated Hangzhou Chest Hospital, Zhejiang University School of Medicine, Hangzhou 310003, China.
Email: hedon114@zju.edu.cn

Funding information
Medicine and Health Science and Technology Plan Projects of Zhejiang Province, Grant/Award Number: 2018KY597

Abstract

Background: Tuberculous pleural effusions (TBPEs) and malignant pleural effusions (MPEs) are two of the most common and severe forms of exudative effusions. Clinical differentiation is challenging; however, metabolomics is a collection of powerful tools currently being used to screen for disease-specific biomarkers.

Methods: 17 TBPE and 17 MPE patients were enrolled according to the inclusion criteria. The normalization gas chromatography-mass spectrometry (GC-MS) data were imported into the SIMCA-P + 14.1 software for multivariate analysis. The principal component analysis (PCA) and orthogonal partial least-squares discriminant analysis (OPLS-DA) were used to analyze the data, and the top 50 metabolites of variable importance projection (VIP) were obtained. Metabolites were qualitatively analyzed using the National Institute of Standards and Technology (NIST) databases. Pathway analysis was performed by MetaboAnalyst 4.0. The detection of biochemical indexes such as urea and free fatty acids in these pleural effusions was also verified, and significant differences were found between these two groups.

Results: 1319 metabolites were screened by non-targeted metabonomics of GC-MS. 9 small molecules (urea, L-5-oxoproline, L-valine, DL-ornithine, glycine, L-cystine, citric acid, stearic acid, and oleamide) were found to be significantly different ($p < 0.05$ for all). In OPLS-DA, 9 variables were considered significant for biological interpretation (VIP≥1). However, after the ROC curve was performed, it was found that the metabolites with better diagnostic value were stearic acid, L-cystine, citric acid, free fatty acid, and creatinine (AUC > 0.8), with good sensitivity and specificity.

Conclusion: Stearic acid, L-cystine, and citric acid may be potential biomarkers, which can be used to distinguish between the TBPE and the MPE.

KEYWORDS
biomarker, GC-MS, malignant pleural effusion, metabolomics, tuberculous pleural effusion

1 | INTRODUCTION

Pleural effusions (PEs) arise from a variety of systemic, inflammatory, infectious, and malignant conditions.[1] When a pleural effusion is considered, efforts should be made to find the cause of the effusion to ensure the appropriate treatment therapy. Pleural effusions may be classified into transudates or exudates based on the mechanism of fluid formation. If the patient has a transudative effusion, the systemic abnormality can be treated and no attention needs to be diverted to the pleura. Alternatively, if an exudative effusion is present

investigations need to be directed toward the pleura to find out the cause of the local problem.[2]

For instance, in China, more than 833 patients with undiagnosed pleural effusions successfully underwent medical thoracoscopy. The study indicated that 40.0% of patients receiving medical thoracoscopy have been confirmed as TBPE, which is much higher than many other countries. Furthermore, the most common undiagnosed pleural effusions are malignant or tuberculous pleural effusions in China.[3] So, in this article, an approach to distinguish TBPEs from MPEs is demonstrated.

Tuberculosis (TB) is a major public health problem in developing countries. TB as the leading cause of deaths has surpassed HIV/AIDS due to an infectious disease.[4] Tuberculous pleuritis (TBP) ranks among the most common forms of extrapulmonary tuberculosis and the most frequent causes of PE.[5] However, if a patient has tuberculous pleuritis, it is important to establish the diagnosis in case of nonstandard treatment, which may lead to a high likelihood of subsequently developing pulmonary or extrapulmonary tuberculosis.[1] Tuberculous pleuritis is widely known to represent primarily a hypersensitivity reaction to tuberculous protein, while the bacillary burden in the pleural space is low.[6,7] For this reason, microbiological analyses are often negative. The diagnosis of TBP is established by showing a pleural effusion ADA level more than 40 IU/L in a lymphocytic pleural effusion.[1] In equivocal cases, needle biopsy or thoracoscopy may be necessary to support the diagnosis. Pleural biopsy is a fast and key method, with high diagnostic efficacy. However, the procedure is invasive and technically difficult.[8] The World Health Organization (WHO) guidelines recommend the use of the tuberculin skin test (TST) and the interferon release assays (IGRAs) as screening tests. The existing screening tests are indirect methods that only provide immunological evidence of host sensitization to Mycobacterium tuberculosis antigens, cannot differentiate accurately between latent tuberculosis infection (LTBI) and active TB, or provide evidence regarding the stage and potential progression from infection to disease.[9] However, commercial IGRAs, performed on either whole-blood or pleural fluid samples, have poor diagnostic accuracy in patients suspected to have TBPE.[10] The Xpert MTB/RIF (Cepheid), a new technology recently endorsed by the WHO, provides high sensitivity for the detection of TB and drug resistance.[11] However, the added value of Xpert MTB/RIF to diagnose pleural or peritoneal TB is limited by its poor sensitivity.[12,13] Therefore, novel and accurate diagnostic strategies are great challenging and in urgent need for early diagnosis of TBPE.

Malignant pleural effusion (MPE) is a common complication of lung cancer, which is the leading cause of cancer mortality in many countries.[14-16] MPE is an exudate in 95% of cases[17,18] and commonly lymphocytic.[19,20] It has also been well documented that tuberculosis and cancer represent the two most frequent causes of exudative PE. TBPEs and MPEs are all predominantly lymphocytic and similar in results of biochemistry and routine examination.[20,21] Moreover, the different PEs can cause similar clinical manifestations. Therefore, the diagnosis of PE is the key for the therapeutic strategies.

In this study, we investigated the patients with TBPEs or MPEs by gas chromatography-mass spectrometry (GC-MS) in China. As a classic chromatographic technique, GC-MS offers strong separation ability, high sensitivity, large peak capacity, excellent repeatability, and stable retention time, which make it an excellent method for identification of biological or pathological variations that occurs in human diseases. This study aimed to explore the metabolic product difference between TBPEs and MPEs in order to find potential markers, which can differentiate cases of TBPEs from MPEs.

2 | MATERIALS AND METHODS

2.1 | Materials

Methanol (HPLC grade), pyridine, methoxyamine hydrochloride, and N-methyl-N-(trimethylsilyl)trifluoroacetamide with 1% trimethylchlorosilane (MSTFA with 1% TMCS) were purchased from Sigma-Aldrich. Distilled water was filtered using a Milli-Q System (Millipore).

2.2 | Study subjects

The study was carried out in Affiliated Hangzhou Chest Hospital, Zhejiang University School of Medicine from October 2017 to May 2018. All the enrolled patients signed the informed contents. The study was approved by the Ethics Committee of the Hospital.

TPE [21,22]:

1. Acid-fast bacilli positive or find Mycobacterium tuberculosis (MTB) in PE sample;
2. Find granulomatous pleurisy on pleural biopsy specimen;
3. PPD skin test positive combined with laboratory examination;
4. Diagnostic antituberculosis treatment is effective.

MPE [21,23]: find malignant cells in PE and/or on closed pleural biopsy specimen. (In our study, all the MPEs are secondary to metastases to the pleura from lung).

The malignant and tuberculous pleurisy groups were confirmed pathologic diagnosis based on pleural biopsy or thoracoscopy, which was established by two different pathologists at least. The patients enrolled are all verified through chest ultrasonic examinations, and all clinical records were available. The patients who had a coexisting systemic disease, immunodeficiency, autoimmune disease, or hemothorax would be excluded from the current investigation. Pleural fluid samples were obtained from these patients. Patients' information details are shown in Table 1. Finally, a total of 34 eligible patients were included in our study.

Pleural fluid samples were centrifuged at 1000 g for 10 min at 4°C. The supernatant was stored in cryovial and kept at −80°C.

2.3 | Pleural fluid sample preparation and GC-MS analysis

The pleural fluid samples were chemically derivatized and then analyzed by GC-MS.[24,25] The sample processing diagram is shown

TABLE 1 The participants and pleural fluid characteristics in the two groups

Baseline	TBPE (n = 17)	MPE (n = 17)	*p*-value
Age (years)	48.88 ± 18.12	75.29 ± 12.6	0.06
Gender (male/female)	13/4	11/6	0.47
Fever (Y/N)	6/11	1/16	0.12
ADA (U/L)	20.64 ± 19.25	8.35 ± 5.80	<0.01
TP (g/L)	46.03 ± 8.81	45.02 ± 12.13	0.24
Glu (mmol/L)	7.11 ± 2.14	5.57 ± 2.92	0.72
AFP (U/L)	1.23 ± 0.64	4.30 ± 12.43	0.08
CEA (μg/L)	1.86 ± 1.37	296.3 ± 481.17	0.00
CA125 (U/L)	577.36 ± 515.17	2347.65 ± 2763.77	0.00
CA153 (U/L)	12.19 ± 6.12	183.01 ± 240.54	0.00

Notes:: A 2-sample analysis of *t* test was used for the group comparison, $p < 0.05$. The exact test was used for categorical data. Data are shown as mean ±SD or ratios.

in Figure 1. 2.0 μL solution was injected in splitless mode into the system after derivatization. The system was an Agilent 7693 Series Autosampler (Agilent Technologies) and an Agilent 7890A GC System equipped with a fused silica capillary column (30 m × 0.25 mm i.d.) chemically bonded to a 0.25 m HP-5MS stationary phase (Phenomenex). The carrier gas helium was used with a constant flow rate of 1.0 mL/min. The injection, ion source, and quadrupole temperatures were 270℃, 230℃, and 150℃, respectively. Optimized conditions are as follows: The initial column temperature was held at 70℃ for 5 min and then ramped at a rate of 15℃/min to 280℃, and maintained for 9 min. The column effluent was introduced into the ion source of an Agilent 5975C Mass Selective Detector (Agilent Technologies). Masses were acquired from m/z 60 to 800.

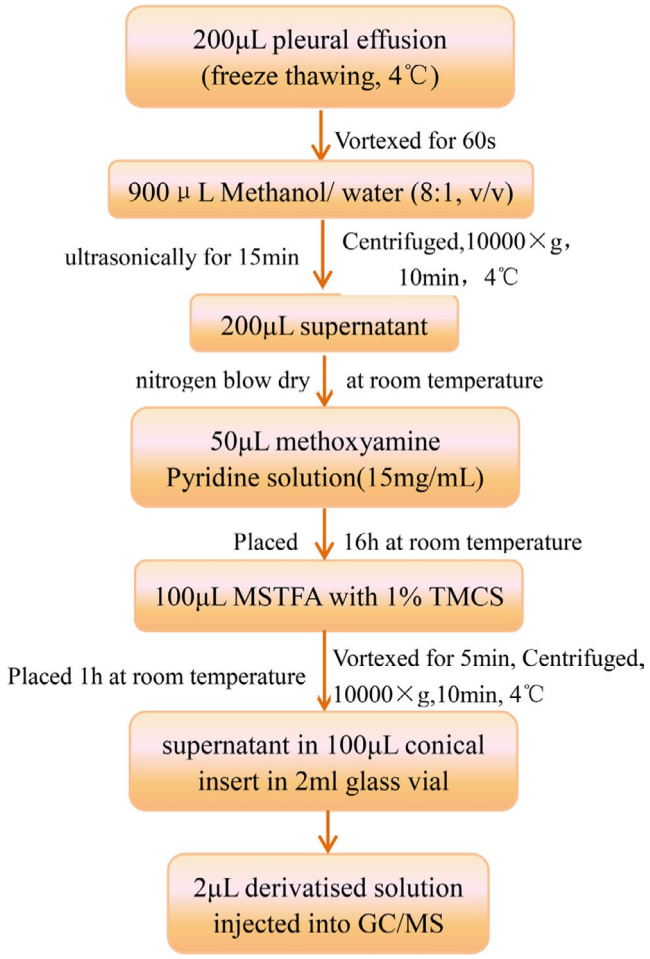

FIGURE 1 Sample processing (methanol/ water: precipitate the protein; methoxyamine and pyridine solution: chemical derivatization of the PE metabolite; MSTFA with 1% TMCS: catalyst)

2.4 | Data processing

Each sample generated a total ion current (TIC). These GC/MS data were analyzed using the "R" software. Sample information, ion intensities, m/z values, and potential markers based on retention time (RT) were obtained after processing. The processed data were multivariate-analyzed by SIMCA-P + 14.1 (Umetrics). An unsupervised PCA assessed the stability and reproducibility of the data. A supervised OPLS-DA was performed to maximize the separation of the groups and generated the general metabolomic trend of pleural fluid. The S plots and variable importance projection (VIP) values derived from OPLS-DA were used to select potential biomarkers. In general, parameters with VIP >1 could have an important influence on inter-group separation. The metabolites were identified by comparing the standard mass fragments in the National Institute of Standards and Technology (NIST) mass spectra library based on >70% similarity index.[26] In addition, MetaboAnalyst 4.0 was used to recognize significant pathways of altered metabolites, which incorporate powerful pathway enrichment analysis and pathway topology analysis.

2.5 | Statistical analysis

A t test was implemented to compare the relative number (peak area) of identified metabolites between TBPE and MPE patients with SPSS software 21.0 (SPSS, Inc.). Data are expressed as mean±standard deviation (SD). $p < 0.05$ was considered to be statistically significant. The diagnostic significance of the metabolites in discriminating the

TBPE patients from the MPE patients was evaluated by an area under the receiver operating characteristic (ROC) curve (AUC), sensitivity, and specificity.

3 | RESULTS

3.1 | Clinical manifestations and clinical characteristics of the PEs

In our study, pleural TB affects mainly younger adults (mean age = 48 years), and those cases may be in the primary stage of the disease. Pleural TB mainly affects male with an overall male-to-female ratio of 1.2:1. TBPE most commonly manifests as an acute or subacute illness causing fever, cough, and pleuritic chest pain in more than 54.6% of patients. Other symptoms include night sweats, weight loss, malaise, and dyspnea varying in severity according to the effusion's size. As a general rule, an acute illness is more likely to occur in younger patients who are more immunocompetent.[7] In contrast, the mean MPEs' age at presentation is 75 years. Dyspnea is the commonest symptom. Patients may also have cough, chest pain, and constitutional symptoms such as weight loss, malaise, and anorexia. Symptoms of the underlying malignancy may also be presented, such as hemoptysis, change in bowel habit, or passage of blood per rectum.[27]

Table 1 displays clinical data from study patients on the basis of the two types of pleural effusions. Significant differences were observed in all parameters between the two groups.

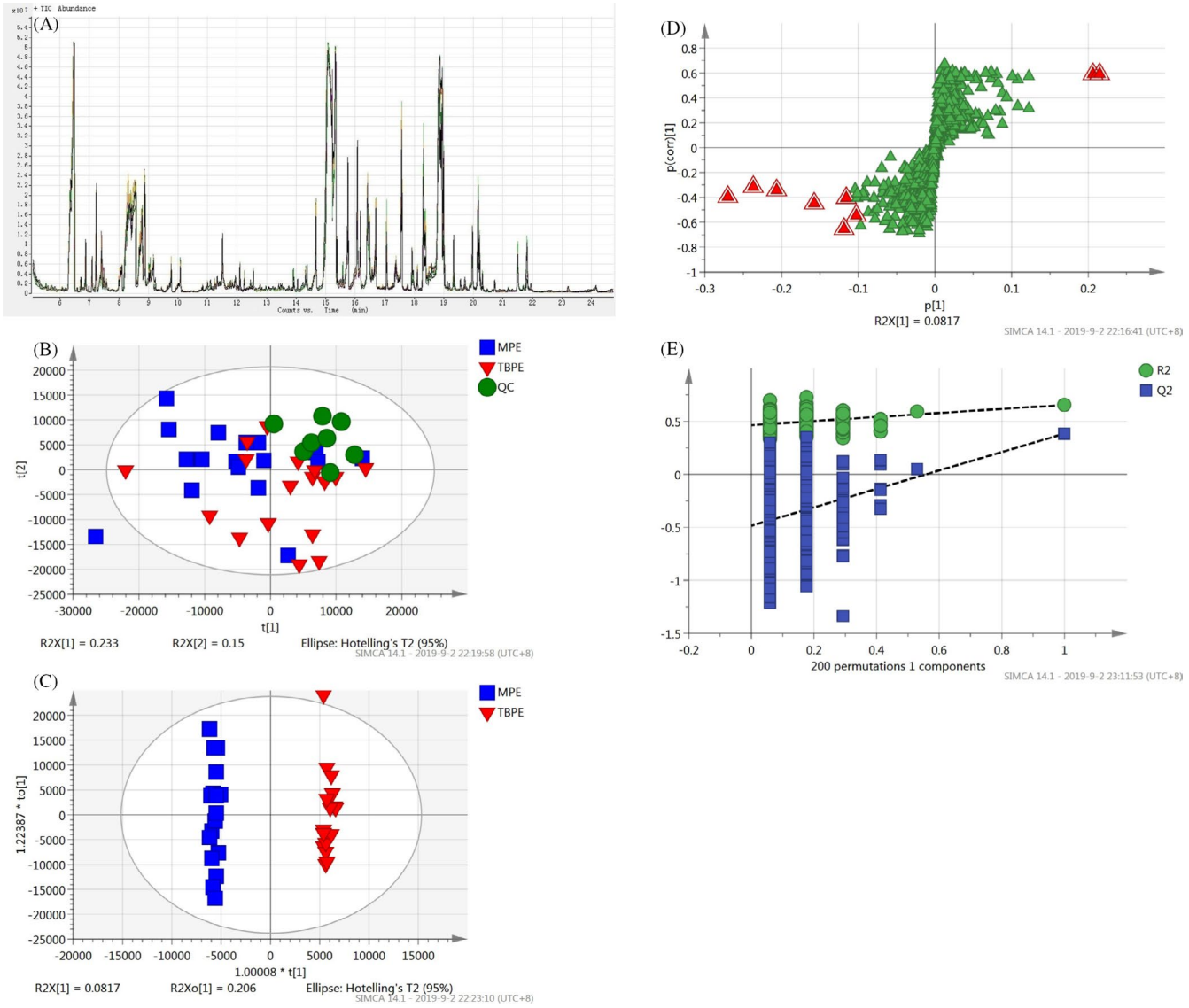

FIGURE 2 (A) Six representative GC-MS TIC chromatograms of the same sample; (B) the PCA score plot; QC samples showed tight clustering, suggesting the GC-MS system to be highly reproducible. (C) The OPLS-DA score plot (R2X (cum) = 0.838, R2Y (cum) = 0.996, Q2 (cum) = 0.303); (D) S plot constructed from the OPLS-DA model. The identified metabolites (red triangles) are farthest from the origin. These metabolites were considered as potential biomarkers and showed marked discrimination of the groups. (E) A permutation test was performed to validate the OPLS-DA model (R2 = 0. 462, Q2 = −0.446)

TABLE 2 Changes in PE levels of 9 key metabolites identified by GC-MS

NO.	RT	MZ	VIP	Match percent (%)	Metabolites	Correlation	Trend	*p*-value
1	514	147.1	9.6531	92.3	Urea	−0.194641	↓	0.020
2	690	156.1	4.01162	80.7	L–5-Oxoproline	−0.137734	↓	0.017
3	485	144.1	3.69541	84	L-Valine	−0.124897	↓	0.012
4	859	142.1	2.90595	82.2	DL-Ornithine	−0.0947709	↓	0.029
5	549	174.1	2.7901	72.8	Glycine	−0.0959028	↓	0.046
6	1086	148.1	2.35037	92.6	L-Cystine	−0.0812039	↓	0.002
7	862	273.1	2.14305	95.3	Citric acid	−0.0709359	↓	0.003
8	1054	203.1	6.8557	83.7	Stearic acid	0.234721	↑	0.000
9	1130	131.1	5.17474	95.4	Oleamide	0.0895687	↑	0.037

Abbreviation: RT, retention time; MZ, mass-to-charge ratio; VIP, variable importance projection; Match percent (%), metabolites and the matching value resulting from the NIST database comparison; Trend: ↓descend compared with the MPE; ↑increased compared with the MPE. VIP >1, variables for the differences in two groups of metabolites; $p < 0.05$, for the difference between the two groups that have statistical significance.

3.2 | Multivariate analysis of GC-MS data

As shown in Figure 2A, six representative GC-MS TIC chromatograms of the same sample showed slight overlaps. The peaks did not exhibit any obvious drift and retention times were stable, which indicated the repeatability and the reliability of measurements.

An extract of each 10 μL sample was prepared as a quality control (QC) sample. The QC samples were disposed and tested in the same manner as the analytic samples. To assess the repeatability of the analysis, the QC samples were injected at regular intervals (every 5 samples). The normalization GC-MS data were imported into the SIMCA-P + 14.1 software for multivariate analysis. 1319 metabolites were screened by non-targeted metabonomics of GC-MS.

To better visualize the subtle similarities and differences among the complex datasets, principal component analyses (PCAs) and orthogonal partial least-squares discriminant analyses (OPLS-DAs) were performed. PCA displays the internal structure of datasets in an unprejudiced manner and compresses multidimensional data into several major components. In the PCA score plot, each data point represents one sample, and the distance between points on the score plot is an indication of the similarity between samples. Examination of the PCA score plots (Figure 2B) provided unsatisfactory separation of data between TBPE and MPE patients. To obtain a higher level of group separation and obtain a better understanding of the variables responsible for classification, supervised OPLS-DA was performed (Figure 2C and D). Subsequently, the parameters for the classification according to the software were R2Y = 0.738 and Q2Y = 0.486, which were stable with good fit and predictive ability. Sevenfold cross-validation was used to estimate the robustness and the predictive ability of our model, and such a permutation test was performed to further validate the model. No overfitting was observed according to the results of the two hundred random permutations, and the R2 and Q2 intercept values were 0. 462 and −0.446, respectively (Figure 2F). As shown in the OPLS-DA score plot, TBPEs were clearly separated from MPEs (Figure 2C), indicating that TBPEs and MPEs had significantly different metabolic profiles.

Potential biomarkers of TBPE and MPE were acquired from the OPLS-DA model according to a VIP value of >1 and $p < 0.05$. Potential biomarkers are shown in the S plot of Figure 2E, and the variables were considered as the greatest potential biomarkers located in the upper far right and lower far left. They played an important role in separating groups and correlations. 24 potential biomarkers with a VIP >1 were selected. The 24 metabolites that contributed to the discrimination were identified.

Only 9 of the 24 discriminant metabolites detected were properly identified by comparing their retention time and the standard mass fragments with those available in the NIST mass spectra library. Nine metabolites had 70% mass spectral similarity with compounds in the NIST library. Those substances with less than 70% similarity index were considered unidentified.[26] The retention time, match percent, and correlation compared with the control are listed in Table 2.

Both PCA and heat map can be used to estimate whether predefined groups form separate or overlapping clusters.[28] Let us look at a dataset about metabolic profiles of TBPE and MPE samples. From the heat map, we can see the average changes of 9 metabolites in the two groups (Figure 3). The different levels of metabolites were quantified by measuring the peak area after normalization. Compared with MPE, the TBPE patients had lower levels of urea, L-5-oxoproline, L-valine, DL-ornithine, glycine, L-cystine, and citric acid. In contrast, the levels of stearic acid and oleamide were significantly higher in TBPEs (Figure 3 and Table 2).

3.3 | Pathway analysis

The path analysis could identify the most relevant path in the research condition using MetaboAnalyst 4.0 [26,29] (https://www.metaboanalyst.ca/MetaboAnalyst/). The identified substances participate in various biological processes, including glycine, serine, and threonine metabolism; citrate cycle (TCA cycle); arginine and proline metabolism; valine, leucine, and isoleucine biosynthesis; and cysteine

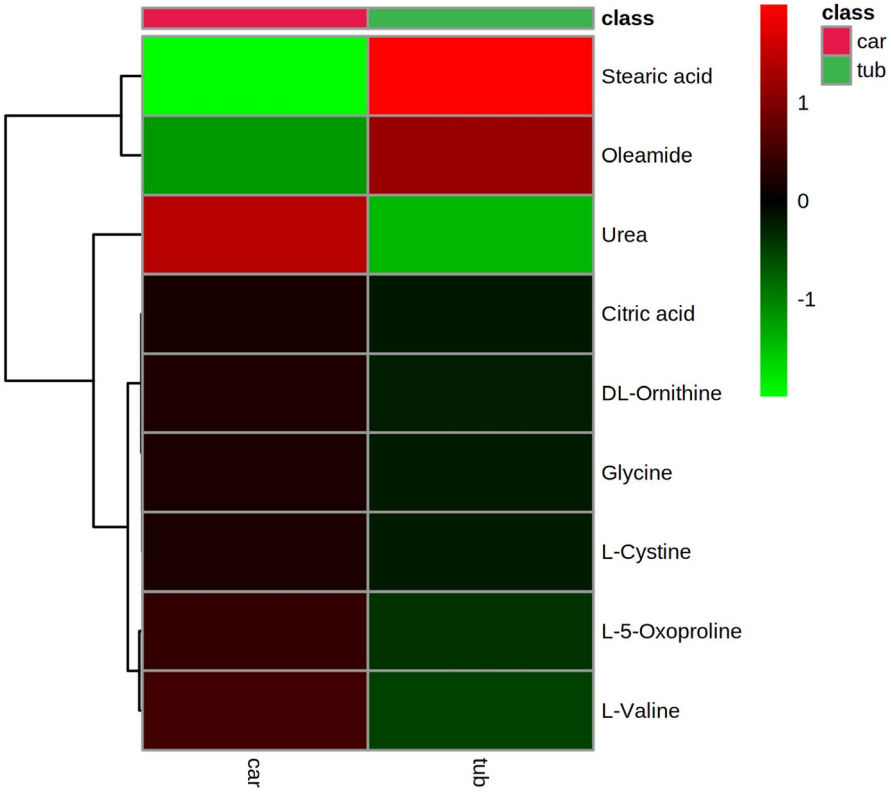

FIGURE 3 Clustering result shown as heat map. There are 9 metabolites in the two groups. Compared with MPE, the TBPE patients had lower levels of urea, L-5-oxoproline, L-valine, DL-ornithine, glycine, L-cystine, and citric acid. The levels of stearic acid and oleamide were significantly higher in TBPEs

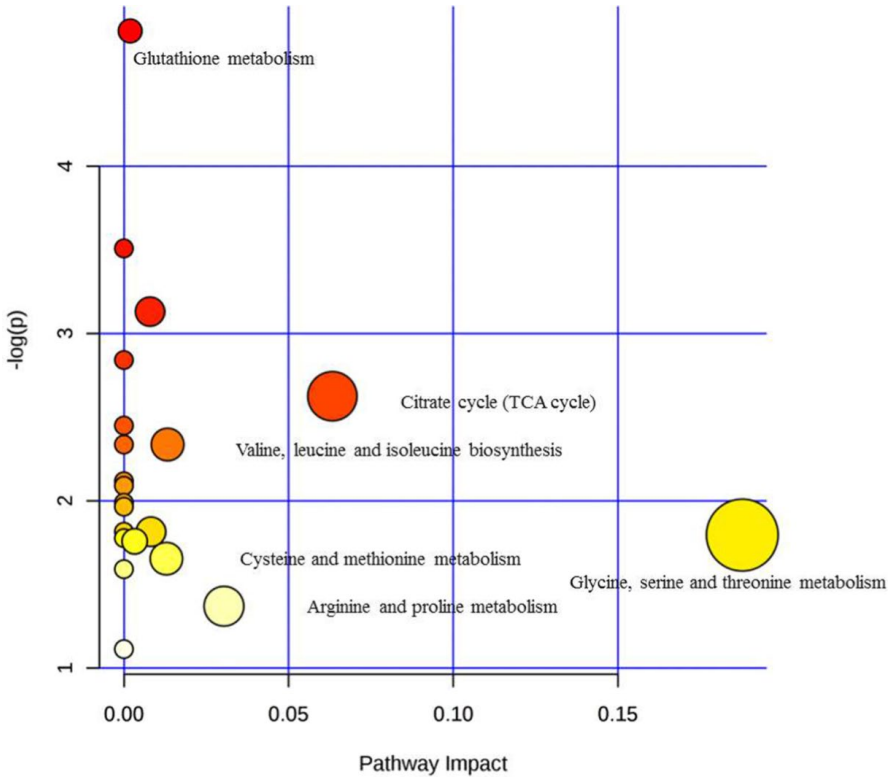

FIGURE 4 Pathway analysis of differential metabolites

and methionine metabolism (Figure 4). However, all the pathways either showed borderline significant differences or did not reach the significance level (p = 0.072, 0.097, 0.166, 0.254, and 0.191, respectively). The metabolic pathways are distributed in the human (Figure 5).

3.4 | Biochemical analysis verification

The body breaks down proteins and amino acids to form nitrogen-containing compounds that are converted into urea in the liver. And nitrogenous waste is toxic. Urea nitrogen refers to the content of N

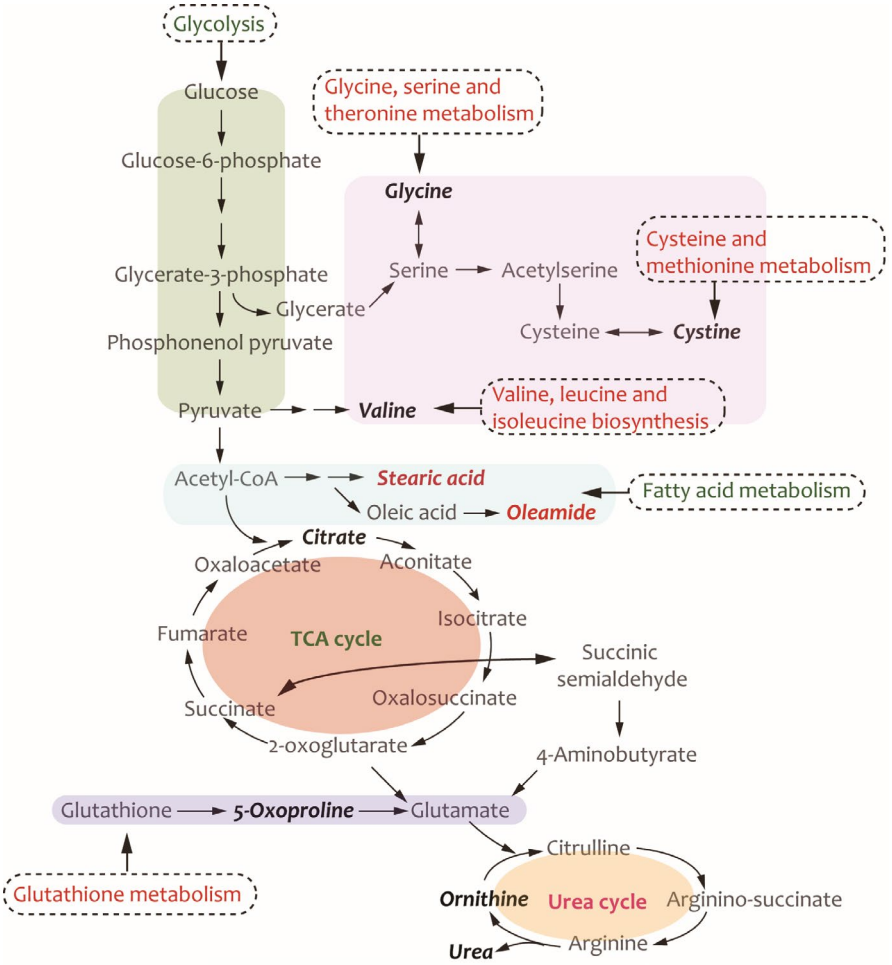

FIGURE 5 The metabolic pathways distributed in the human. Metabolic pathways are included glycine, serine, and threonine metabolism; cysteine and methionine metabolism; valine, leucine, and isoleucine biosynthesis; fatty acid metabolism; the tricarboxylic acid (TCA) cycle; urea cycle; and glutathione metabolism. Black italic, significantly decreased; red italic, significantly increased

in urea molecular amino group. The results showed that there were statistical differences (Table 3).

3.5 | Diagnostic value of concentrations of the metabolites for discriminating TBPE and MPE patients.

Finally, based on ROC curves, we evaluated the diagnostic significance of the metabolites for distinguishing TBPE from MPE. The AUCs of stearic acid, L-cystine, citric acid, urea, L-valine, DL-ornithine, and L-5-oxoproline were 0.855, 0.827, 0.848, 0.747, 0.734, 0.706, and 0.709, respectively (Figure 6A and B, Tables 4 and 5). There was no significant difference in diagnostic value between oleamide and glycine, and the *p*-values were 0.06 and 0.07, respectively. With an optimal calculated free fatty acid threshold of 103 mmol/L, the AUC was 0.881, with a sensitivity and specificity of 94% and 77%, respectively. With creatinine threshold of 70.75 mmol/L, the AUC was 0.860, with a sensitivity and specificity of 88% and 71%, respectively (Figure 6C, Table 6).

TABLE 3 Biochemical detection data of substances in pleural effusion

Baseline	TPE (n = 17)	MPE (n = 17)	*p*-value
Uric acid (μmol/L)	205.75 ± 75.56	285.05 ± 71.93	0.004
Creatinine (μmol/L)	65.79 ± 13.82	95.85 ± 29.08	0.001
Urea nitrogen (mmol/L)	3.91 ± 1.31	6.21 ± 2.21	0.001
Free fatty acid (mmol/L)	99.5 ± 36.94	167.23 ± 54.62	0

Notes:: A 2-sample analysis of *t* test was used for the group comparison, $p < 0.05$. The exact test was used for categorical data. Data are shown as mean ±SD or ratios.

4 | DISCUSSION

In clinical practice, TBPEs and MPEs are the two frequent exudative PE.[1,30] TBPE is one of the most common forms of extrapulmonary tuberculosis. Differential diagnosis of TPE from PE with the other etiologies, especially MPE, is always a diagnostic challenge.

The present study focused on the small molecular profile using a GC-MS measurement, and the differences in the signal intensities of the small molecules between tuberculosis and malignancy pleural effusions were observed. In the current study, a total of nine small molecules were found to be significantly different between the two effusions ($p < 0.05$ for all), especially urea, stearic acid, and oleamide (Figure 3). In OPLS-DA, nine variables (urea, L-5-oxoproline, L-valine, DL-ornithine, glycine, L-cystine, citric acid, stearic acid, and

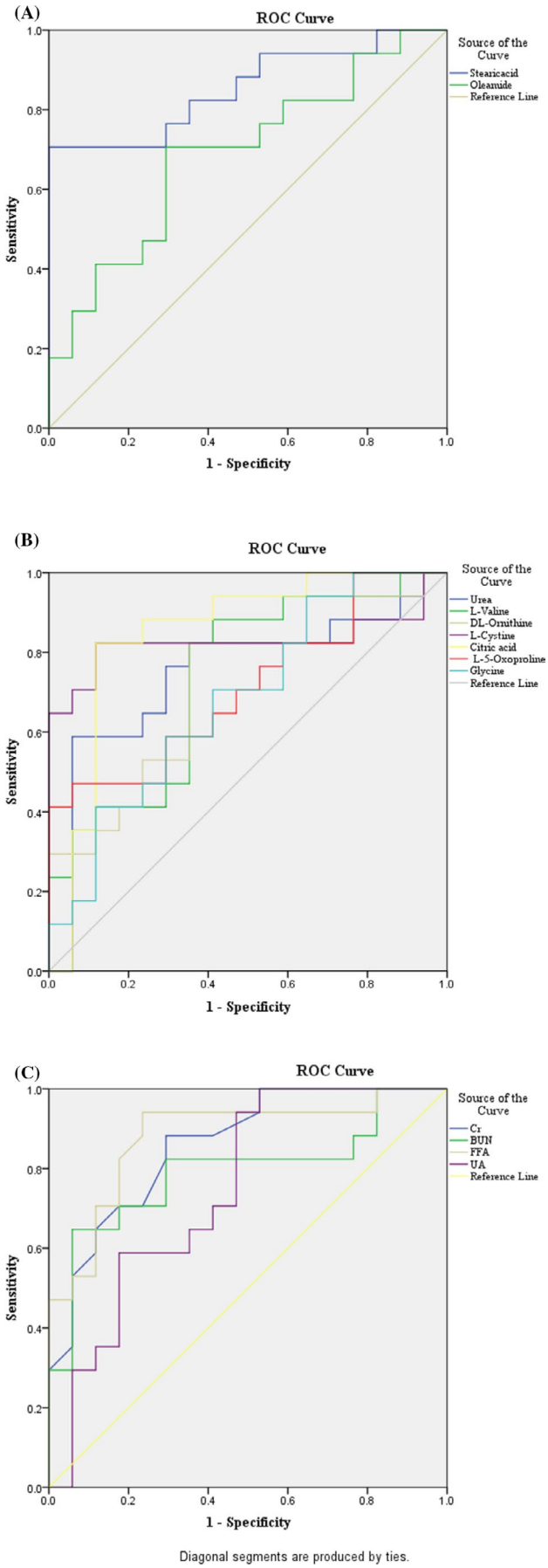

FIGURE 6 ROC curves of pleural effusion concentrations of stearic acid, oleamide, urea, L-5-oxoproline, L-valine, DL-ornithine, glycine, L-cystine, citric acid, uric acid, creatinine, urea nitrogen, and free fatty acid for discriminating TPE patients from MPE patients. (A) ROC curves of pleural effusion concentrations of stearic acid and oleamide. (B) ROC curves of pleural effusion concentrations of urea, L-5-oxoproline, L-valine, DL-ornithine, glycine, L-cystine, and citric acid. (C) ROC curves of pleural effusion concentrations of uric acid, creatinine, urea nitrogen, and free fatty acid. *Note*: A used TPE as cases and MPE as controls. B and C used MPE as cases and TPE as controls

oleamide) were considered significant for biological interpretation (VIP≥1), especially urea, stearic acid, and oleamide.

The difference in signal pathway analysis of metabolites was not obvious. This may suggest that there are some similarities between tuberculous and malignant pleural effusion in the development of the disease. Both diseases consume a lot of energy and nutrients. Except for urea metabolism and stearic acid and oleamide metabolism, there are great differences.

Urea and ornithine were the products of urea cycle (UC). The complete UC took place in the liver. Hepatocytes process toxic ammonia produced upon the metabolism of proteins and amino acids through a series of biochemical reactions that yield urea, a disposable by-product that was excreted in the urine. Mounting evidence suggests that UC intermediates were shunted to anabolic routes in cancer. Multiple types of tumors exhibit altered expression levels in UC components, which was associated with reduced generation of nitrogen waste and increased redirection of carbon and nitrogen to biosynthetic routes. Indeed, the tight crosstalk of the UC with other metabolic routes implied that aberrant expression in nearly every enzyme within this cycle was potentially capable of redirecting UC metabolites to support tumor growth. In turn, the UC provides an excellent example of an emerging feature of cancer cells: the context-dependent metabolic flexibility that enables optimal use of metabolic resources, maximizing biosynthesis and economizing carbon and nitrogen waste.[31] In the study, the signal intensity of both urea and ornithine in MPEs was significantly higher than that in TBPEs, suggesting some relations might exist between urea /ornithine and tumor; however, further researches to clarify those relations are still required. Furthermore, the detection results of urea nitrogen in pleural effusion showed a significant statistical difference.

Stearic acid with a carbon chain length of 18 markedly inhibited the activity of chymase, which is the main protein in mast cell granules. Furthermore, it was postulated to be important in the inflammatory reaction.[32] As expected, a significant increase in signal intensity of stearic acid was observed in the TBPEs.

Stearic acid played a pro-inflammatory role in a variety of cells through Toll-like receptor 4.[33] The accumulation of stearic acid in macrophages could induce the expression of inflammatory factors mediated by Toll-like receptor 4, which leads to endoplasmic reticulum stress-mediated apoptosis.[34] Stearic acid could induce the expression of CD11c on macrophages through epidermal fatty acid-binding protein, thus promoting the antigen presentation and inflammatory cytokine release of macrophages.[35]

TABLE 4 Diagnostic significance of pleural effusion concentrations of stearic acid and oleamide for discriminating TPE patients from MPE patients

Variable	Sensitivity (%)	Specificity (%)	Cutoff value	AUC	*p*-value
Stearic acid	71	100	20594042	0.855	0*
Oleamide	71	71	25977351.5	0.689	0.06*

Abbreviation: AUC, area under the curve.

*Represents a *p*-value less than 0.05.

TABLE 5 Diagnostic significance of pleural effusion concentrations of urea, L-5-oxoproline, L-valine, DL-ornithine, glycine, L-cystine, and citric acid for discriminating TPE patients from MPE patients

Variable	Sensitivity (%)	Specificity (%)	Cutoff value	AUC	*p*-value
Urea	0.59	0.94	3908473.500	.747	0.014*
L-Valine	0.82	0.65	7246403.610	.734	0.020*
DL-Ornithine	0.82	0.65	1785036.100	.706	0.040*
L-Cystine	0.82	0.88	1142841.160	.827	0.001*
Citric acid	0.82	0.88	1014795.520	.848	0.001*
L–5-Oxoproline	0.47	0.94	7847607.200	.709	0.037*
Glycine	0.94	0.35	4774336.520	.682	0.071

Abbreviation: AUC, area under the curve.

*Represents a *p*-value less than 0.05.

Oleamide was an endogenous fatty acid amide.[36] It had been found that oleamide was activated by inhibiting nuclear transcription factor (NF-κ B) in mouse microglia. Activated oleamide could inhibit the expression of inducible nitric oxide synthase (iNOS) and cyclooxygenase-2 (COX-2) induced by lipopolysaccharide (LPS), and then inhibit the release of pro-inflammatory mediators NO and prostaglandin E2.[37] Oleamide inhibited the release of inflammatory mediators and pro-inflammatory cytokines induced by LPS by inhibiting the mitogen-activated protein kinase (MAPK) signaling pathway and NF-κB signaling pathway in macrophages.[38] This was consistent with the inflammatory reaction of tuberculosis pleural effusion. Moreover, the detection results of free fatty acids in pleural effusion showed that there was a significant statistical difference.

Pathway analysis using MetaboAnalyst 4.0 was an extension of the metabolite set enrichment analysis with extra procedures to calculate the impact on the pathways based on network topology analysis. However, all the metabolic pathways showed no reach the significance level. The results might indicate that there were some similarities in metabolism between TBPE and MPE.

Abundant evidence also indicates the metabolites not only participates in the pathogenesis of TBPE and MPE, but also can be a complementary tool to distinguish between the TBPE and MPE, except oleamide and glycine. We also measured uric acid, creatinine, urea nitrogen, and free fatty acid as some of the metabolic pathway products and consistently found significant differentiation in TBPE patients from MPE patients.

TABLE 6 Diagnostic significance of pleural effusion concentrations of uric acid, creatinine, urea nitrogen, and free fatty acid for discriminating TPE patients from MPE patients

Variable	Sensitivity (%)	Specificity (%)	Cutoff value	AUC	*p*-value
Cr	0.88	0.71	70.75	.860	0.000*
BUN	0.65	0.94	5.77	.792	0.004*
FFA	0.94	0.77	103	.881	0.000*
UA	1	0.47	175.5	.747	0.014*

Abbreviations: AUC, area under the curve; BUN, blood urea nitrogen; Cr, creatinine; FFA, free fatty acid; UA, uric acid.

*Represents a *p*-value less than 0.05.

4.1 | Limitations of the study

To the best of our knowledge, many differential variables between patients with TBPE and MPE have yet to be identified, and their identification may have been limited by the sample size and single metabolomic technology platform used in this study. Further investigations consisting of larger sample sizes and a combination of multiple analytical platforms are warranted to validate our results.

The difference in stearic acid, L-cystine, and citric acid is more obvious between TBPEs and MPEs. The biochemical indexes in pleural effusion verified that there were significant differences in urea and free fatty acids between the two groups.

5 | CONCLUSION

The present GC/MS-based metabonomic approach focused on the small molecules provided a rapid and sensitive method to differentiate TBPEs from MPEs. A combination of the small molecules is performed as novel biomarkers in the effusions such as stearic acid, L-cystine, and citric acid to discriminate the TBPEs from MPEs. The results that revealed simultaneous detection of changes in multiple metabolites using GC-MS exerted a significant advantage over conventional clinical examinations. Now, the further comparison of larger clinical samples to determine the real applicability of the current GC/MS-based metabonomic approach is undergoing in our laboratory.

ACKNOWLEDGEMENTS

We thank the patients who participated in the study. This work was supported by grants from the Medicine and Health Science and Technology Plan Projects of Zhejiang Province (Grant Number 2018KY597).

CONFLICT OF INTEREST

The authors declare no competing financial interests.

DATA AVAILABILITY STATEMENT

The data that support the findings of this study are available from the corresponding author upon reasonable request.

ORCID

Yongxia Liu https://orcid.org/0000-0003-0364-5835

REFERENCES

1. Light RW. Pleural effusions. *Med Clin North Am*. 2011;95:1055-1070.
2. Porcel JM, Azzopardi M, Koegelenberg CF, et al. The diagnosis of pleural effusions. *Expert Rev Respir Med*. 2015;9:801-815.
3. Wang XJ, Yang Y, Wang Z, et al. Efficacy and safety of diagnostic thoracoscopy in undiagnosed pleural effusions. *Respiration*. 2015;90:251-255.
4. Glaziou P, Floyd K, Raviglione MC. Global epidemiology of tuberculosis. *Semin Respir Crit Care Med*. 2018;39:271-285.
5. Skouras VS, Kalomenidis I. Pleural fluid tests to diagnose tuberculous pleuritis. *Curr Opin Pulm Med*. 2016;22:367-377.
6. Light RW. Update on tuberculous pleural effusion. *Respirology*. 2010;15:451-458.
7. Porcel JM. Tuberculous pleural effusion. *Lung*. 2009;187:263-270.
8. Wong CF. Early diagnosis of tuberculous pleural effusion: apart from pleural fluid adenosine deaminase, pleural biopsy still has a role. *Hong Kong Medical Journal*. 2018;24:316-317.
9. Matteelli A, Sulis G, Capone S, et al. Tuberculosis elimination and the challenge of latent tuberculosis. *Presse Med*. 2017;46:e13-e21.
10. Aggarwal AN, Agarwal R, Gupta D, Dhooria S, Behera D. Interferon gamma release assays for diagnosis of pleural tuberculosis: a systematic review and meta-analysis. *J Clin Microbiol*. 2015;53:2451-2459.
11. Boehme CC, Nabeta P, Hillemann D, et al. Rapid molecular detection of tuberculosis and rifampin resistance. *N Engl J Med*. 2010;363:1005-1015.
12. Tadesse M, Abebe G, Bekele A, et al. Xpert MTB/RIF assay for the diagnosis of extrapulmonary tuberculosis: a diagnostic evaluation study. *Clin Microbiol Infect*. 2019;25:1000-1005.
13. Penz E, Boffa J, Roberts DJ, et al. Diagnostic accuracy of the Xpert(R) MTB/RIF assay for extra-pulmonary tuberculosis: a meta-analysis. *Int J Tuberc Lung Dis*. 2015;19:278-284, i–iii.
14. Jemal A, Bray F, Center MM, et al. Global cancer statistics. *Ca-a Cancer Journal for Clinicians*. 2011;61:69-90.
15. Park JY, Jang SH. Epidemiology of lung cancer in Korea: recent trends. *Tuberc Respir Dis (Seoul)*. 2016;79:58-69.
16. Siegel RL, Miller KD, Jemal A. Cancer statistics, 2016. *CA Cancer J Clin*. 2016;66:7-30.
17. Ashchi M, Golish J, Eng P, O'Donovan P. Transudative malignant pleural effusions: prevalence and mechanisms. *South Med J*. 1998;91:23-26.
18. Ryu JS, Ryu ST, Kim YS, Cho JH, Lee HL. What is the clinical significance of transudative malignant pleural effusion? *Korean J Intern Med*. 2003;18:230-233.
19. Verma A, Dagaonkar RS, Marshall D, Abisheganaden J, Light RW. Differentiating malignant from tubercular pleural effusion by cancer ratio plus (cancer ratio: pleural lymphocyte count). *Can Respir J*. 2016;2016:7348239.
20. Na MJ. Diagnostic tools of pleural effusion. *Tuberc Respir Dis (Seoul)*. 2014;76:199-210.
21. Liu Q, Yu YX, Wang XJ, Wang Z, Wang Z. Diagnostic accuracy of interleukin-27 between tuberculous pleural effusion and malignant pleural effusion: a meta-analysis. *Respiration*. 2018;95:469-477.
22. Gopi A, Madhavan SM, Sharma SK, Sahn SA. Diagnosis and treatment of tuberculous pleural effusion in 2006. *Chest*. 2007;131:880-889.
23. Lepine PA, Thomas R, Nguyen S, et al. Simplified criteria using pleural fluid cholesterol and lactate dehydrogenase to distinguish between exudative and transudative pleural effusions. *Respiration*. 2019;98:48-54.
24. Chen E, Lu J, Chen D, et al. Dynamic changes of plasma metabolites in pigs with GalN-induced acute liver failure using GC-MS and UPLC-MS. *Biomed Pharmacother*. 2017;93:480-489.
25. Yu K, Sheng G, Sheng J, et al. A metabonomic investigation on the biochemical perturbation in liver failure patients caused by hepatitis B virus. *J Proteome Res*. 2007;6:2413-2419.
26. Musharraf SG, Mazhar S, Choudhary MI, Rizi N. Atta ur R: Plasma metabolite profiling and chemometric analyses of lung cancer along with three controls through gas chromatography-mass spectrometry. *Sci Rep*. 2015;5:8607.
27. Asciak R, Rahman NM. Malignant pleural effusion: from diagnostics to therapeutics. *Clin Chest Med*. 2018;39:181-193.
28. Metsalu T, Vilo J. ClustVis: a web tool for visualizing clustering of multivariate data using principal component analysis and heatmap. *Nucleic Acids Res*. 2015;43(W1):W566-W570.
29. Yu H, Zhao Y, Zhang Y, Zhong L. Metabolic profiling of acromegaly using a GC-MS-based nontargeted metabolomic approach. *Endocrine*. 2020;67(2):433-441.
30. Ferreiro L, Toubes ME, San Jose ME, et al. Advances in pleural effusion diagnostics. *Expert Rev Respir Med*. 2020;14:51-66.
31. Keshet R, Szlosarek P, Carracedo A, Erez A. Rewiring urea cycle metabolism in cancer to support anabolism. *Nat Rev Cancer*. 2018;18:634-645.
32. Kido H, Fukusen N, Katunuma N. Inhibition of chymase activity by long chain fatty acids. *Arch Biochem Biophys*. 1984;230:610-614.
33. Miao H, Chen L, Hao L, et al. Stearic acid induces proinflammatory cytokine production partly through activation of lactate-HIF1alpha pathway in chondrocytes. *Sci Rep*. 2015;5:13092.
34. Anderson EK, Hill AA, Hasty AH. Stearic acid accumulation in macrophages induces toll-like receptor 4/2-independent inflammation leading to endoplasmic reticulum stress-mediated apoptosis. *Arterioscler Thromb Vasc Biol*. 2012;32:1687-1695.
35. Zeng J, Zhang Y, Hao J. Stearic acid induces CD11c expression in proinflammatory macrophages via epidermal fatty acid binding protein. *J Immunol*. 2018;200:3407-3419.
36. Mendelson WB, Basile AS. The hypnotic actions of the fatty acid amide, oleamide. *Neuropsychopharmacology*. 2001;25:S36-39.
37. Oh YT, Lee JY, Lee J, et al. Oleamide suppresses lipopolysaccharide-induced expression of iNOS and COX-2 through inhibition of NF-kappaB activation in BV2 murine microglial cells. *Neurosci Lett*. 2010;474:148-153.
38. Moon SM, Lee SA, Hong JH, et al. Oleamide suppresses inflammatory responses in LPS-induced RAW264.7 murine macrophages and alleviates paw edema in a carrageenan-induced inflammatory rat model. *Int Immunopharmacol*. 2018;56:179-185.

How to cite this article: Liu Y, Mei B, Chen D, Cai L. GC-MS metabolomics identifies novel biomarkers to distinguish tuberculosis pleural effusion from malignant pleural effusion. *J Clin Lab Anal*. 2021;35:e23706. https://doi.org/10.1002/jcla.23706